(15) Whangbo, M. H.; Hoffmann, R. *J. Am. Chem. Soc.* **1978**, *100*, 6093.
(16) Dewar, M. J. S.; Dougherty, R. C. *The PMO Theory of Organic Chemistry*; Plenum: New York, 1975.
(17) Carey, F. A.; Sundberg, R. J. *Advanced Organic Chemistry Part A*, 2nd ed.; Plenum: New York, 1984; pp 37-51.
(18) Fleming, I. *Frontier Orbitals and Organic Chemical Reactions*; Wiley: London, 1976.
(19) Durkin, K. A.; Langler, R. F. *J. Phys. Chem.* **1987**, *91*, 2422. Eichel, W.; Luthe, H.; Matter, Y. M.; Michaelis, W.; Boldt, P. *J. Org. Chem.* **1987**, *52*, 205. Kost, D.; Aviram, K. *J. Am. Chem. Soc.* **1986**, *108*, 2006. Pitea, D.; Gastaldi, M.; Orsini, F.; Pelizzoni, F.; Mugnoli, A.; Abbondanti, E. *J. Org. Chem.* **1985**, *50*, 1853.
(20) See for example: Reference 16, p 88.
(21) Longuet-Higgins, H. C. *Phys. Rev.* **1950**, *18*, 265, 275, 283.
(22) Wennerstrom, O. *Macromolecules* **1985**, *18*, 1977.
(23) Lahti, P.; Obrzut, J.; Karasz, F. E. *Macromolecules* **1987**, *20*, 2023.
(24) Whangbo, M.-H.; Hoffmann, R.; Woodward, R. B. *Proc. R. Soc. London, A* **1979**, *366*, 23.
(25) Diaz, A. F.; Crowley, J.; Baryon, J.; Gardini, G. P.; Torrance, J. B. *J. Electroanal. Chem. Interfacial Electrochem.* **1981**, *121*, 355.
(26) Shacklett, L. W.; Chance, R. R.; Ivory, D. M.; Miller, G. G.; Baughman, R. H. *Synth. Met.* **1979**, *1*, 307.
(27) Kovacic, P.; Hsu, L. *J. Polym. Sci. Polym. Chem. Ed.* **1966**, *4*, 5.
(28) McKean, D. R.; Stille, J. K. *Macromolecules* **1987**, *20*, 1787.
(29) *The Sadtler Handbook of Ultraviolet Spectra*; Simons, W. W., Ed.; Sadtler: Philadelphia, PA, 1979.
(30) Silverstein, R. M.; Bassler, G. C.; Morrill, T. C. *Spectrometric Identification of Organic Compounds*, 4th ed.; Wiley: New York, 1981.
(31) Wheland, G. W. *Resonance in Organic Chemistry*; Wiley: New York, 1955; p 333.
(32) Salem, L. *The Molecular Orbital Theory of Conjugated Systems*; Benjamin: New York, 1966; p 154.
(33) Maier, J.; Turner, D. W. *Faraday Discuss. Chem. Soc.* **1972**, *No. 54*, 149.
(34) Kossmehl, G.; Yaridjanian, A. *Makromol. Chem.* **1981**, *182*, 3419.
(35) Watanabe, K. *J. Chem. Phys.* **1957**, *26*, 542.
(36) Clar, E.; Schmidt, W. *Tetrahedron* **1978**, *34*, 3219.
(37) Sato, N.; Seki, K.; Inokuchi, H. *J. Chem. Soc., Faraday Trans. 2* **1981**, *77*, 1621.
(38) Samuelson, L.; Batra, I. P.; Roetti, C. *Solid State Commun.* **1980**, *33*, 817.
(39) Dujardin, F.; Decruppe, J. P. *J. Phys. (Les. Ulis, Fr.)* **1981**, *42*, 1167.
(40) Dillon, R. O.; Spain, I. L.; McClure, J. W. *J. Phys. Chem. Solids* **1977**, *38*, 635.
(41) Painter, G. S.; Ellis, D. E. *Phys. Rev. B: Solid State* **1970**, *1*, 4747.
(42) Greenway, D. L.; Harbeke, G.; Bassani, F.; Tosatti, E. *Phys. Rev.* **1969**, *178*, 1340.
(43) Tanaka, K.; Yamashita, S.; Yamabe, H.; Yamabe, T. *Synth. Met.* **1987**, *17*, 143.

Permeability-Controllable Membranes. 9.[1] Electrochemical Redox-Sensitive Gate Membranes of Polypeptide Films Having Ferrocene Groups in the Side Chains[2]

Yoshio Okahata* and Kazuya Takenouchi

Department of Polymer Chemistry, Tokyo Institute of Technology, Ookayama, Meguro-ku, Tokyo 152, Japan. *Received April 20, 1988; Revised Manuscript Received July 1, 1988*

ABSTRACT: Poly(γ-methyl-L-glutamate-*co*-γ-(ferrocenylmethyl)-L-glutamate) (PMLG–Fc(x), x = 6–100%) and poly(γ-tetradecyl-L-glutamate-*co*-γ-(ferrocenylmethyl)-L-glutamate) ($PC_{14}LG$–Fc(x), x = 6–98%) were prepared from poly(γ-methyl-L-glutamate). Permeation of water-soluble fluorescent probes through PMLG–Fc(x) films cast on a platinum minigrid sheet was enhanced by a factor of 1–5 by an electrochemical oxidation of a ferrocenyl (Fc) unit in the side chains, compared with that of the reduced form. Permeability could be changed reversibly at least 20 cycles by repeated redox reactions. The extent of rate enhancements (P_{ox}/P_{red}) depended on the content of Fc side chains. Upon oxidation of Fc to Fc^+ side chains in the film α-helical conformations of polypeptide chains decreased and permeants could diffuse easily in the hydrophilic Fc^+ side-chain region or the disordered random coil polypeptide region. In the case of the $PC_{14}LG$–Fc(x) film containing both ferrocene and long alkyl chain groups in side chains, permeability was regulated by both electrochemical redox reactions and temperature changes (melting of side chains). When the anionic (NS^-, NS^{2-}, and NS^{3-}) and cationic (NA^+ and NA^{2+}) probes were employed as a permeant, storage and release phenomena of permeants were observed due to the electrostatic interaction with Fc^+ cations in the film by redox reactions. When the vinyl polymer having ferrocenyl groups in side chains (PFcAc) was employed as a cast film on a Pt grid, redox-sensitive permeability changes were not observed.

Biological membranes are mainly composed of lipid bilayer matrices, proteins incorporated either in the interior or on the surface, and polysaccharides adsorbed mainly on the surface. Lipid bilayers and protein molecules play important roles in the transport of specific substrates and are considered to form a "hole" or a "channel" across the membrane by molecular conformational changes responding to external stimuli.

As a model of lipid bilayer matrices, we have prepared some kinds of permeability-controllable artificial lipid membranes: a multibilayer-corked capsule membrane,[3-5] a monolayer-immobilized porous glass plate,[6,7] and a multibilayer-immobilized cast film.[1,8-10] Permeability across these artificial lipid assemblies supported by the physically strong membranes could be changed reversibly, responding to various outside effects such as temperature changes (phase transition), photoirradiation, ambient pH changes, electric field, and protein interactions.[11] These permeability controls could be explained by orientation changes of lipid matrices responding to external stimuli.

As a structural model of membrane proteins, synthetic polypeptide films have been prepared so that their permeability by the conformational change of the helical structure or the side-chain mobility could be regulated.[12-19] For example, the permeability of poly(glutamic acid)-containing polymer membranes can be affected by the conformational changes of α-helical polypeptide segments responding to ambient pH changes.[12-14] The ion permeability and membrane potential of polypeptide membranes having photoresponsive groups such as azobenzene in side

0024-9297/89/2222-0308$01.50/0

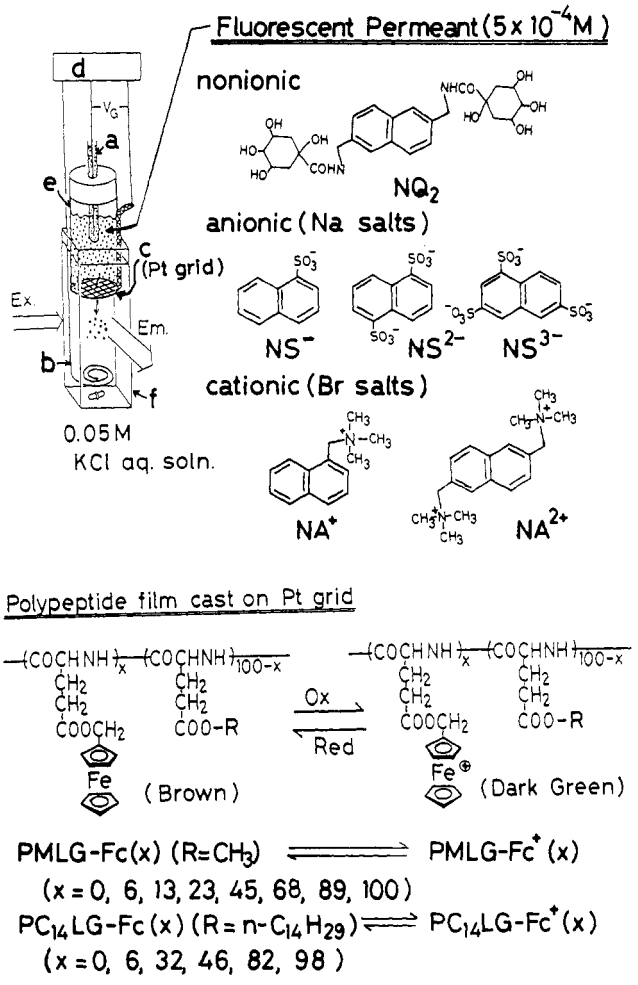

Figure 1. Experimental setup for permeation of fluorescent probes through redox-type polypeptide films cast on a Pt minigrid sheet. (a) Reference electorde, Ag/AgCl in saturated KCl (–0.05 V versus SCE); (b) Pt wire for counter electrode; (c) Pt minigrid sheet (100 mesh, 70 μm thick, and 28-mm² area) embedded in polypeptide films; (d) potentiostat; (e) polyethylene tube; (f) 1-cm quartz cell.

chains can be reversibly changed by photoirradiation due to the cis–trans photoisomerization of azobenzene groups in side chains.[15,16,18] Polypeptide films containing thiol groups in the side chains can be ion permeability regulated by a chemical oxidative reaction.[19]

In this paper, we describe that electrochemical potentials can also act as a stimuli which causes the reversible permeation changes of the synthetic polypeptide membrane. Poly(glutamate ester)s having various amounts of ferrocenylmethyl groups in side chains [PMLG–Fc(x)] were prepared by an ester exchange method from poly(γ-methyl-L-glutamate). $PC_{14}LG$–Fc(x) having both ferrocene and long tetradecyl alkyl groups in side chains were also prepared. The polypeptide film was cast on a Pt minigrid sheet and permeation of water-soluble substances through the film was followed fluorophotometrically by switching on and off an electrical potential applied on a Pt grid/film. A schematic illustration of the permeation apparatus and the structures of polypeptides and permeants are shown in Figure 1. Freely water-soluble fluorescent probes (nonionic NQ_2; anionic NS^-, NS^{2-}, and NS^{3-}; cationic NA^+ and NA^{2+}) were used as a permeant.

Permeation control of chloride anions by electrochemical redox reactions was first achieved by Burgmayer and Murray[29,30] by using a conductive polypyrrole film deposited on a Au grid sheet. The electrochemical binding and release of various anions and a cation from polypyrrole films on an electrode have been recently reported by several groups.[31-36]

Experimental Section

Materials. Preparations of freely water-soluble nonionic [2,6-bis[(1,3,4,5-tetrahydroxycyclohexanecarboxamido)methyl]-naphthalene (NQ_2)], cationic [1-(trimethylammoniomethyl)-naphthalene bromide (NA^+) and 2,6-bis(trimethylammoniomethyl)naphthalene dibromide (NA^{2+})], and anionic [sodium naphthalene-1-sulfonate (NS^-), disodium naphthalene-1,5-disulfonate (NS^{2-}), and trisodium naphthalene-1,3,6-trisulfonate (NS^{3-})] fluorescent permeation probes were reported elsewhere.[20] Poly(γ-methyl-L-glutamate) was used without further purification which was presented from Aji-no-moto Co., Tokyo (average D_p = 2500).

Poly(γ-methyl-L-glutamate-*co*-γ-(ferrocenylmethyl)-L-glutamate) [PMLG–Fc(x)] was prepared by an ester exchange reaction of poly(γ-methyl-L-glutamate) (PMLG) and excess amounts of ferrocenylmethyl alcohol[21] (mp 47–76 °C) in 1,2-dichloroethane at 70 °C for 2–10 h in the presence of a small amount of concentrated H_2SO_4. The polymer was repeatedly reprecipitated from 1,2-dichloroethane with excess of methanol to remove unreacted ferrocenylmethyl alcohol. The content (x%) of ferrocenylmethyl groups in the polymer side chain was regulated by the feed of ferrocenylmethyl alcohol in exchange reactions and determined by elemental analyses (C, H, N, and Fe).

Poly(γ-tetradecyl-L-glutamate-*co*-γ-(ferrocenylmethyl)-L-glutamate) [$PC_{14}LG$–Fc(x)] was prepared as follows. Poly(γ-tetradecyl-L-glutamate) was obtained by an ester exchange reaction of PMLG with a large excess amount of tetradecanol according to literature.[22] The polymer was purified by repeated reprecipitation from 1,2-dichloroethane with excess of methanol. It was confirmed by ^1H and ^{13}C NMR spectra and elemental analyses (C, H, and N) that γ-methyl groups were converted more than 98% to C_{14} side chains. The obtained $PC_{14}LG$ was converted to $PC_{14}LG$–Fc(x) by the ester-exchange reaction with ferrocenylmethyl alcohol in a similar manner as PMLG–Fc(x). The experimental conditions and results are summarized in Table I.

Poly(ferrocenylmethyl acrylate) (PFcAc) was prepared by a radical polymerization of the respective monomer (mp 56–59 °C)

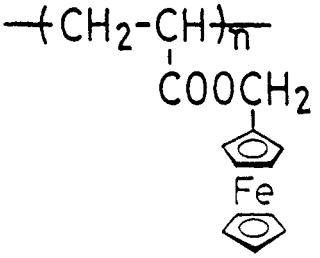

PFcAc

in benzene in the presence of 2,2′-azobis(isobutyronitrile) at 70 °C for 90 h. The polymer was purified by reprecipitation from benzene with excess of *n*-hexane. Average degree of polymerization was estimated to be 2×10^4 by gel permeation chromatography.

The structures and purities of obtained polymers were confirmed by ^1H NMR, ^{13}C NMR, and IR spectroscopy and elemental analyses (C, H, N, and Fe).

Characterization of Polypeptide Films. The polymers, PMLG–Fc(x) (x = 0, 6, 13, 23, 45, 68, 89, 100), $PC_{14}LG$, $PC_{14}LG$–Fc(x) (x = 0, 6, 32, 46, 82, 98), and PFcAc were dissolved in chloroform (0.6 wt %). When the solution was spread on a flat glass plate and dried, the film was enough physically strong to be detached from the glass plate.

Circular dichroism (CD) spectrum of films were measured by using a Jasco J-20A spectropolarimeter. CD spectra of the reduced and oxidized films cast on a quartz plate were taken in distilled water before and after immersing them into an aqueous solution of cerium(IV) ammonium nitrate (oxidizing reagent) for 5 min.

Absorption spectra of the film were measured with a Shimazu UV-240 spectrophotometer. The film cast with 1 μm thick on the inner surface of a UV cell and filled with distilled water was measured in both the reduced and oxidized forms before and after

Table I
Preparations and Characterizations of Poly(glutamate) Containing Ferrocene Side Groups

polymers	ferrocenylmethyl alcohol in feed, g (mmol)[a]	Fc content, %[b]	rel content of α-helix conform[c]	
			red form	ox form
PMLG		100	100	
PMLG–Fc(6)	0.15 (0.7)	6.4	82	74
PMLG–Fc(13)	0.3 (1.4)	13.2	62	44
PMLG–Fc(23)	0.5 (2.3)	23.4	40	13
PMLG–Fc(45)	1.3 (6.0)	45.3	38	14
PMLG–Fc(68)	1.4 (6.3)	68.2	36	14
PMLG–Fc(89)	2.0 (9.3)	88.9	35	4.9
PMLG–Fc(100)	5.0 (23)	99.5	32	12
$PC_{14}LG$		100	100	
$PL_{14}LG$–Fc(6)	0.33 (1.5)	6.1	98	95
$PL_{14}LG$–Fc(32)	0.5 (2.3)	31.8	87	65
$PL_{14}LG$–Fc(46)	0.67 (3.0)	46.4	75	42
$PL_{14}LG$–Fc(82)	1.66 (7.7)	81.9	40	20
$PL_{14}LG$–Fc(98)	5.0 (23)	98.7	32	12

[a] Poly(γ-methyl-L-glutamate), 0.87 g (6.0 unit mmol), or poly(γ-tetradecyl-L-glutamate), 0.50 g (1.5 unit mmol); solvent, 1,2-dichloroethane 100 mL, concentrated H_2SO_4 0.1 mL. [b] Obtained by Fe content from elemental analyses. [c] Estimated roughly from ellipticity at 222 nm of circular dichroism spectra.

immersing aqueous Ce(IV) ions for 5 min, respectively.

IR spectra of the film cast on a KRS plate (TlBr and TlI) were carried out by using a Jasco IR-1800 spectrometer.

Differential scanning calorimetry (DSC) of the $PC_{14}LG$–Fc(x) film was carried out with a Daini-Seiko-Sha Model SSC-560 instrument. A small piece of the film was sealed with 50 μL of distilled water in an Ag-sample pan and heated from 5 to 90 °C at a rate of 2 °C min^{-1}.

Cyclic voltammetric studies of the ferrocene-containing films cast on a Pt wire as a working electrode were carried out in N_2-purged 0.05 M KCl aqueous solution using a three-electrode potentiogalvanostat (Nikko Keisoku Co., Model NPGFZ-2501). A platinum wire and Ag/AgCl in saturated KCl (−0.05 V versus SCE) were used as the counter and reference electrodes, respectively.

Permeation Measurements. The chloroform solution (0.6 wt %) of polymers was cast on a platinum minigrid sheet (100 mesh, 70 μm thick) attached at the bottom of a polyethylene tube as shown in Figure 1. The film was transparent, physically strong, and water-insoluble. The film thickness was estimated to be 100 ± 5 μm from the scanning electron micrograph observation.

Fluorescent probes were dissolved in 0.05 KCl aqueous solution (5.0×10^{-4} M) and stored in the upper cell in Figure 1. Permeation through the film/grid (28-mm^2 area, 100-μm thickness) was followed fluorophotometrically in the lower cell at 340 nm (excited at 280 nm) in 0.05 M KCl aqueous solution. The aqueous solution was O_2-degassed and N_2-purged before each experiment. The relative permeation coefficient, P (cm^2 s^{-1}), was obtained from the following equation:[1,6-10]

$$P = Jd/C_0S \quad (1)$$

where d and S are a thickness and an area of the film, respectively. J and C_0 are a flux of permeation (a slope of Figure 3) and an initial concentration of the probe in the upper cell, respectively.

Permeation experiments were carried out upon applying the potential +0.5 V and 0 V versus SCE to the Pt grid/film in order to oxidize and reduce a ferrocene unit in the film, respectively. The reference electrode (Ag/AgCl/aqueous KCl) and the counter Pt wire were set in the upper and the lower aqueous solution in the cell, respectively, as shown in Figure 1. The same potentiogalvanostat was used as that in cyclic voltammetric studies. Since the upper probe solution is not stirred during experiments, the small amount of concentration polarization of the probe may be considered, which makes the measured permeability lower than actual.

The decomposition and quenching of fluorescent probes were not detected under applying a potential of −0.5 to +0.7 V on the Pt grid/film during permeation experiments. Since the reference electrode and the counter electrode are on opposite sides of the dividing minigrid sheet, the potential of the working electrode may not show the correct value. When the Pt counter electrode was set in the upper solution with the reference electrode, however, the fluorescence intensity was markedly reduced and the permeation of probes was not constant, probably because probes were electrochemically oxidized or reduced. However, the reliable and reproducible permeation results were obtained, when three electrodes were set up as shown in Figure 1.

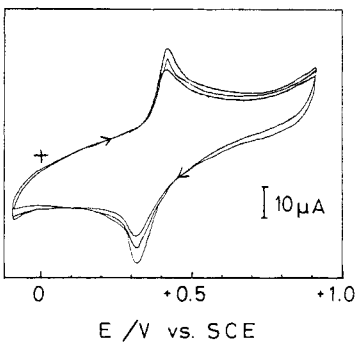

Figure 2. Cyclic voltammograms of the PMLG–Fc(45) film cast on a Pt wire in 0.05 M KCl aqueous solution. Sweep rate: 50 mV s^{-1}.

Results and Discussion

Cyclic Voltammograms of Films. Figure 2 shows a typical cyclic voltammic curve of the PMLG–Fc(45) film cast on a Pt wire in N_2-purged 0.05 M KCl aqueous solution with a scan rate of 50 mV s^{-1}. The curve indicates the chemically reversible one-electron oxidation and reduction steps: E_{pa} = +0.42 V versus SCE in anodic region (Fc to Fc^+) and E_{pc} = +0.32 V versus SCE in cathodic region (Fc^+ to Fc). The difference of potential between the oxidation and reduction peaks (electrochemical irreversibility) shows that the reaction does not follow the Nernst equilibrium prediction because of the high resistance of the film. Shapes of cyclic voltammic curves hardly changed at least for 5 min under these sweep rates in the range of 20–50 °C. Other PMLG–Fc(x) and $PC_{14}LG$–Fc(x) films (x = 6–100) showed the similar cyclic voltammic curves (E_{pa} = 0.42 ± 0.03 and E_{pc} = 0.32 ± 0.03 V versus SCE). Peak top currents in both anodic and cathodic regions decreased with decreasing the content of Fc groups in side chains of polypeptide cast films. The vinyl polymer containing Fc groups in all side chains (PFcAc) also showed similar cyclic voltammic curves.

Redox reactions on the film were also confirmed by electronic spectra. When the PMLG–Fc(45) cast film soaked in an aqueous solution of cerium(IV) ammonium nitrate (oxidizing reagent, 0.1 M), the film turned from

Table II
Redox-Sensitive Permeation Rate Constants of Nonionic NQ_2 Probes through Polypeptide Films

polymers	temp, °C	P, 10^{-8} cm^2 s^{-1} red Fc form	ox Fc^+ form	re-red Fc form	P_{ox}/P_{red}[a]
PFcAc	30	24.2	23.0	24.0	1.1
PMLG	30	0.914	0.955	0.940	1.1
PMLG–Fc(6)	30	2.30	2.25	2.28	1.0
PMLG–Fc(13)	30	3.31	3.80	3.33	1.1
PMLG–Fc(23)	30	2.00	2.95	2.05	1.5
PMLG–Fc(45)	30	4.80	25.1	4.95	5.2
PMLG–Fc(68)	30	9.33	31.6	9.40	3.4
PMLG–Fc(89)	30	11.7	28.8	10.9	2.5
PMLG–Fc(100)	30	33.7	87.6	34.5	2.6
$PC_{14}LG$	30	<0.001	<0.001	<0.001	
	50	2.58	2.86	2.78	1.1
$PC_{14}LG$–Fc(6)	30	<0.001	<0.001		
	50	1.58	2.51	1.62	1.6
$PC_{14}LG$–Fc(46)	30	3.98	24.0	3.85	6.0
	50	31.6	44.7	32.0	1.4
$PC_{14}LG$–Fc(98)	30	30.5	88.3	33.5	2.9
	50	105	158	103	1.5

[a] The extent of rate enhancement by the oxidation.

brown to dark green (λ_{max} = 260, 380, and 630 nm) which agrees with the absorption spectrum for Fc^+ cations.[23] After immersing the $Na_2S_2O_4$ aqueous solution (reducing reagent, 0.1 M), the film reverted from dark green to brown (λ_{max} = 290 and 380 nm). When the PMLG–Fc(45) film cast on SnO_2/glass transparent electrode was oxidized and reduced electrochemically by applying +0.5 and 0 V versus SCE, respectively, similar spectral changes were observed. These results indicate that the ferrocene groups in side chains of polypeptide can be reversibly oxidized and reduced in the film.

Redox-Sensitive Permeation of PMLG–Fc(x) Films. Figure 3 shows typical time courses of permeation of the nonionic water-soluble fluorescent probe NQ_2 through the PMLG–Fc(x) film (x = 0, 23, 45, 100) cast on a Pt minigrid sheet under an intermittent redox potential applied to the Pt grid/film. Permeations of the NQ_2 probe was followed fluorophotometrically in an N_2-purged 0.05 M KCl aqueous solution (see Figure 1). A nonionic permeant was chosen to avoid the effect of electrostatic interaction and repulsion with the grid/film.

The permeability was relatively slow in the reduced form of PMLG–Fc(x) films. Upon applying the potential +0.5 V versus SCE to the Pt grid/film, the film turned from brown to dark green immediately which means the oxidation of ferrocene (Fc) to ferricinium cations (Fc^+) and then permeability of NQ_2 probes increased within 30 s by a factor of 1–5, depending on the Fc content of the film. When the potential on the Pt grid/film was switched off to 0 V, even after 10 min in the oxidized form, the dark green PMLG–Fc^+ film was reduced to the brown PMLG–Fc film and permeability reverted to the original slow rate within 30 s. Permeability changes of these PMLG–Fc/PMLG–Fc^+ films (x = 23–100%) on a Pt grid could be reproduced repeatedly at least 20 cycles without damaging the film chemically and physically.

The permeability of PMLG–Fc(x) films increased with increasing the content of Fc side chains in polypeptides and the permeation change due to redox reactions was clearly observed in PMLG–Fc(45) and –Fc(110) films. In contrast, the permeability of the PMLG film having no Fc side groups was very slow and not affected by redox reactions. When the polyvinyl-type film (PFcAc) was employed, the permeability was relatively fast and hardly affected by redox reactions. This indicates that the polypeptide structure and Fc side chains are important to change permeability by redox reactions.

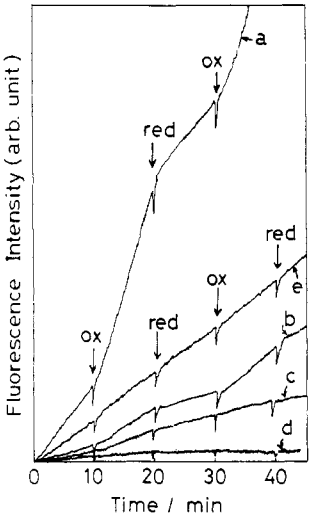

Figure 3. Typical redox-sensitive permeation changes of the nonionic NQ_2 probes through (a) PMLG–Fc(100), (b) PMLG–Fc(45), (c) PMLG–Fc(23), (d) PMLG, and (e) PFcAc films followed fluorophotometrically. The potential 0.5 and 0 V versus SCE was applied to the Pt grid/film at ox and red, respectively.

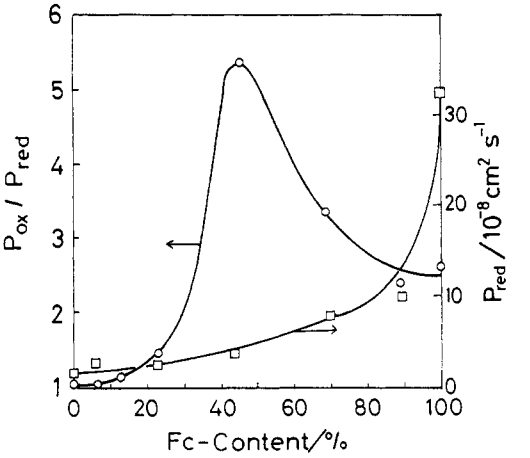

Figure 4. Dependence of the permeation rate in the reduced form (P_{red}) and the rate enhancement by the oxidation (P_{ox}/P_{red}) on the content of ferrocene (Fc) side chains of PMLG–Fc(x) films.

The permeation rate constant, P (cm^2 s^{-1}), was calculated from slopes of Figure 3 from eq 1. Permeation measurements were carried out three times in each experiment

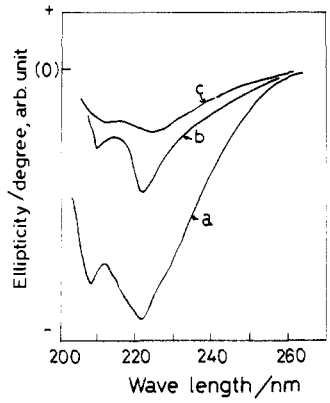

Figure 5. Circular dichroism spectra of (a) the PMLG, (b) the reduced form, and (c) the oxidized form of the PMLG–Fc(45) film in distilled water at 25 °C.

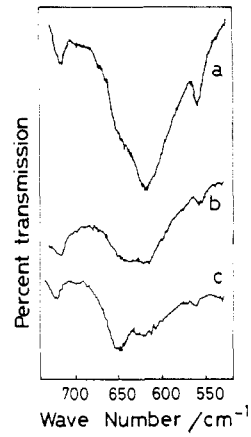

Figure 6. Infrared spectra of (a) the PMLG, (b) the reduced form, and (c) the oxidized form of the PMLG–Fc(45) film.

(deviation ±10%) and the average P value was summarized in Table II. As shown in Figure 4, the permeation rate in the reduced form increased simply with increasing the content of Fc groups in side chains, but the extent of permeation enhancement (P_{ox}/P_{red}) by the oxidation increased with increasing the Fc content of side chains and gave a maximum at 45% of Fc content in the film.

α-Helix Structures in Films. Poly(glutamate ester) is known to take α-helical conformation of polypeptide chains in the film as well as a homogeneous solution.[12-19,24] Figure 5 shows the circular dichroism (CD) spectra of PMLG–Fc(x) films in distilled water. The CD spectrum of the oxidized film was taken in distilled water after immersing it into a Ce(IV) aqueous solution for 5 min. The CD spectrum of the PMLG film showed a strong negative curve at 222 and 208 nm, which indicates that poly(glutamate) chains take mainly right-handed α-helical conformations in the film. In the case of the reduced form of the PMLG–Fc(45) film, the intensity of CD spectrum decreased relatively. When the film was oxidized, the ellipticity at 222 and 208 nm decreased greatly compared with that of the reduced form and reverted to nearly the original intensity by the reduction of the film in $Na_2S_2O_4$ aqueous solution. Thus, PMLG–Fc(45) chains take partly α-helical structures in a similar manner as the homopolymer of PMLG in the film, and the oxidation of Fc side chains decreased the α-helical conformation of polypeptide chains.

Figure 6 shows the part of IR spectra of the PMLG and the PMLG–Fc(45) films in reduced and oxidized forms. Similar results were obtained as those obtained from CD spectra. The PMLG film showed a strong absorption at 620 cm^{-1}, which also indicates polypeptide chains like mainly an α-helical structure in the film.[12-14,25,26] In the case of the reduced form of the PMLG–Fc(45) film, the absorption at 620 cm^{-1} decreased and a new absorption appeared at 650 cm^{-1}, which indicates the random coil structure of polypeptide chains.[25,26] Upon oxidation of the PMLG–Fc(45) film, the absorption at 650 cm^{-1} increased greatly and the 620-cm^{-1} absorption decreased. This means also that the oxidation of Fc side chains decreases α-helical structures of polypepetide chains in the film.

The homopolymer of PMLG was supposed to take a 100% α-helical conformation of the polypeptide chains in the film and the relative extent of α-helical structure of PMLG-Fx(x) films was roughly estimated from the relative maximum value of ellipticity at 222 nm from the CD spectra of Figure 5 and shown in Table I. The α-helical conformations of polypeptide chains changed to random-coil conformations with increasing Fc content in the side chains. Moreover, the oxidation of Fc groups in side chains accelerated the formation of random-coil conformations of PMLG–Fc(x) films.

Permeation Mechanisms. Permeation changes by redox reactions on a Pt minigrid sheet can be explained as follows from the above structural data of PMLG–Fc(x) polypeptide films. In solid membranes of synthetic polypeptides, permeants are thought to diffuse not in the rigid helical skeleton but in the relatively fluid side-chain region. Permeation through PMLG–Fc(x) films increased with increasing Fc group content in side chains (Figure 4 and Table II). Polypeptide chains begin to take the disordered random coil structure instead of the rigid α-helical conformation with increasing the content of bulky Fc side groups and the permeant can easily diffuse through the random-coil region. Upon the oxidation of the PMLG–Fc(x) film, the lipophilic Fc side chain is changed to the hydrophilic Fc^+ cationic groups and the α-helical conformation is distorted by the formation of swelled Fc^+ groups or the electrostatic repulsion between cationic Fc^+ side chains. The water-soluble permeant NQ_2 can easily diffuse and permeate through the hydrophilic and swelled side-chain region or the random coiled polypeptide chain regions. The redox reaction of Fc side chains is plausible to occur in the small part of the film near the Pt grid, because it is difficult to accomplish complete oxidation or reduction in the 100-μm-thick film in the short time of permeation experiments. However, the tiny redox reaction in the film seems to be effective to change the peptide conformation and the probe permeation.

The extent of the permeation enhancement (P_{ox}/P_{red}) by the oxidation of the film showed the maximum at x = 45% in PMLG–Fc(x) films (see Figure 4). The P_{ox}/P_{red} value increased with increasing the Fc content below x = 45% because the effect of the redox reaction on permeation increases with the Fc content in the film. At the higher Fc content above x = 45%, the P_{ox}/P_{red} value decreased with the Fc content. This is explained by the fact that at high content of Fc side chains the permeability of the reduced film increased largely due to the random-coil conformation of polypeptide chains and the effect of the oxidation apparently decreased.

The micromosaic and heterogeneous structure (rigid helical skeleton and fluid side chain region) of polypeptide membranes is important in the redox-sensitive permeation, because a cast film of PFcAc vinyl polymers showed little permeation change upon redox reactions on a Pt grid (see Table II and Figure 3).

Temperature-Sensitive Permeation of $PC_{14}LG$–Fc(x) Films. Poly(glutamate), having long n-alkyl side chains, is known to have thermotropic properties.[22,27,28]

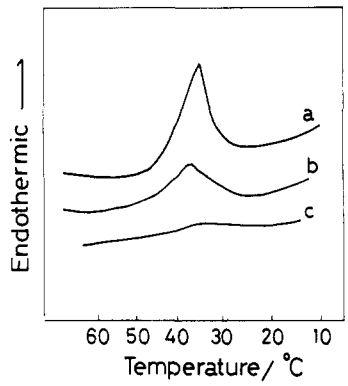

Figure 7. Differential scanning calorimetric curves of (a) $PC_{14}LG$–Fc(6), (b) $PC_{14}LG$–Fc(45), and (c) $PC_{14}LG$–Fc(98) films in distilled water. Scanning speed: 2 °C min^{-1}.

Long alkyl side chains produce a paraffin-like crystal around α-helical polypeptide chains and melt with increasing temperatures. Figure 7 shows the differential scanning calorimetry (DSC) of $PC_{14}LG$–Fc(x) (x = 6, 46, 98) films in aqueous solution. The endothermic peak was observed at 37 °C, indicating the melting of tetradecyl side chains around α-helical polypeptide chains in the case of the $PC_{14}LG$–Fc(6) film as well as a homopolymer of $PC_{14}LG$. The enthalpy change (the peak area) at 37 °C decreased with decreasing the content of long alkyl chains: ΔH = 0.78, 0.45, and 0.020 kcal mol^{-1} for PMLG–Fc(6), –Fc(46), and –Fc(98) films, respectively.

The $PC_{14}LG$–Fc(x) polymers having both long C_{14} alkyl and Fc groups in side chains showed CD spectra similar to those of the PMLG–Fc(x) films in Figure 5: the intensity of a negative curve at 222 and 208 nm decrease with increasing the content of bulky Fc side chains and by the oxidation of Fc groups. The relative α-helical conformation content was calculated roughly from the ellipticity at 222 nm of a homopolymer of $PC_{14}LG$ as a standard (see Table I). The extent of α-helical conformations of $PC_{14}LG$–Fc(x) films is larger than that of PMLG–Fc(x) films in all range of Fc content. Long alkyl chain may help to form rigid α-helical conformation of polypeptides compared with short methyl groups even when the amount of bulky Fc groups increased in side chains. The α-helical extent of $PC_{14}LG$–Fc(x) films did not change in the range 10–60 °C, independent of the melting of C_{14} side chains.

Permeation of NQ_2 probes through $PC_{14}LG$–Fc(x) films could be reversibly regulated by repeated redox reactions on a Pt grid as well as through PMLG–Fc(x) films. The permeability and the extent of rate enhancement (P_{ox}/P_{red}), however, were largely affected by temperatures. Arrhenius plots of permeation rates in both the reduced and oxidized forms of $PC_{14}LG$–Fc(6), –Fc(46), and –Fc(100) films are shown in Figure 8. Numbers in the figure are activated energies (E_a, kcal mol^{-1}), calculated from each slope of the Arrhenius plots. When the $PC_{14}LG$–Fc(6) film having a small amount of Fc groups and a large amount of long alkyl chains was employed, the permeability was very slow ($P < 10^{-11}$ cm^2 s^{-1}) below 37 °C and drastically enhanced at temperatures above 37 °c. This is explained by the melting of paraffin-like side chain regions at 37 °C and permeants diffuse smoothly through fluid liquid regions around α-helical polypeptide backbones. The permeation change responding to redox reactions were small above 37 °C because of the low content of Fc side chains. The activation energy of permeation through the disordered oxidized membrane was smaller than that through the rigid reduced form.

In the case of $PC_{14}LG$–Fc(46) film, the permeability of the reduced form increased incontinuously near 37 °C,

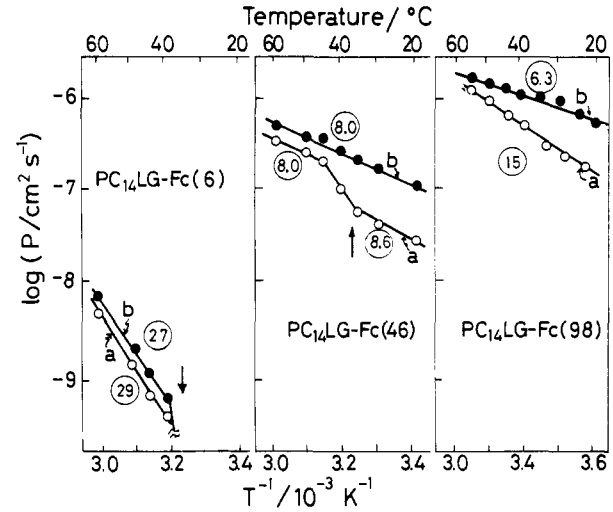

Figure 8. Arrhenius plots of permeation of nonionic NQ_2 probes through (a) the reduced and (b) the oxidized form of $PC_{14}LG$–Fc(x) films (x = 6, 46, and 98). Arrows shows the melting point of C_{14} alkyl side chains in the film. Numbers in the circle indicate the activation energy (E_a, kcal mol^{-1}) calculated from each slope.

responding to the melting of the 54% content of long alkyl side chains. The permeability of the oxidized film enhanced compared with that of the reduced form at all the temperatures and increased linearly with temperature. Since the side-chain region is already disturbed by the formation of hydrophilic Fc^+ cations, the permeability of the oxidized film may not be affected by the melting of C_{14} side chains. The E_a value (8.0 kcal mol^{-1}) for the permeation through the disturbed membranes such as the oxidized film and the reduced film above 37 °C is smaller than that for the solidified, reduced film below 37 °C (E_a = 8.6 kcal mol^{-1}). The large rate enhancement by redox reactions (P_{ox}/P_{red}) was consequently observed in the solidified film below 37 °C rather than in the melting state above 37 °C (see Table II).

In the case of the $PC_{14}LG$–Fc(98) film, in which almost all of alkyl side chains were substituted by Fc groups, permeability of both the reduced and oxidized films was relatively extensive and increased linearly with temperatures. The activation energy for the oxidized form (6.3 kcal mol^{-1}) was very small compared with that for the reduced film (15 kcal mol^{-1}). This also suggests that NQ_2 probes easily permeate through the swelled and disordered side-chain region or the random-coil region of the oxidized film relative to the rigid Fc side-chain regions.

Storage and Release Phenomena of Ionic Permeants. Since the oxidation of PMLG–Fc(x) films on a Pt minigrid sheet produces cationic Fc^+ groups in the film, permeation of charged fluorescent probes such as anionic (NS^-, NS^{2-}, and NS^{3-}) and cationic probes (NA^+ and NA^{2+}) may be affected by the electrostatic interaction with cationic Fc^+ groups in the film. Figure 9 shows typical time courses of permeation changes of dianionic NS^{2-} and dicationic NA^{2+} probes through the PMLG-Fc(45) film under applying +0.5 V and 0 V versus SCE on the Pt grid/film, together with the results of nonionic NQ_2 probes.

When the nonionic NQ_2 probe was employed as a permeant, the permeability enhanced simply within 30 s by oxidation (stage 2) and reverted to the original slow rate by the reduction of the film (stage 4). In contrast, the permeation of the dianionic NS^{2-} probe decreased by oxidation and increased largely by the reduction of the film and the permeability changes were complex. In the case of dicationic NA^{2+} probes, the permeability increased by oxidation with a time lag and then decreased gradually.

Table III
Permeation Changes of Charged Probes through the PMLG–Fc(45) Film by Redox Reactions

permeants	P, 10^{-6} cm^2 s^{-1} red Fc form stage 1	ox Fc^+ form stage 2	ox Fc^+ form stage 3	re-red Fc form stage 4	re-red Fc form stage 5	P_{ox2}/P_{red1}	P_{red4}/P_{ox2}
nonionic							
NQ_2	4.80	25.1		4.95		5.2	0.20
anionic							
NS^-	5.04	0.822	2.37	46.3	5.52	0.16	56
NS^{2-}	6.38	0.780	4.70	63.4	7.57	0.12	81
NS^{3-}	5.82	0.451	1.32	85.6	6.32	0.078	190
cationic							
NA^+	5.46	55.3	7.54	6.08		10	0.11
NA^{2+}	6.04	72.0	13.4	6.54		12	0.091

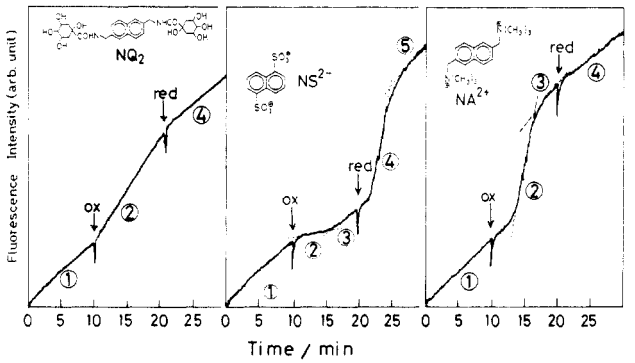

Figure 9. Complex, redox-sensitive permeation changes through the PMLG–Fc(45) film depending on the charge of permeants (nonionic NQ_2, dianionic NS^{2-}, and dicationic NA^{2+} probes). Permeation was followed fluorophotometrically. The potential 0.5 and 0 V versus SCE was applied to the Pt grid/film at ox and red, respectively.

Permeation rates calculated from each slope of Figure 9 were summarized in Table III, together with those of mono- and trianionic (NS^- and NS^{3-}) and monocationic (NA^+) probes.

The complex permeation phenomena of ionic probes in Figure 9 can be explained as follows. In the case of the anionic probe permeation, cationic Fc^+ charges produced by the oxidation accumulate anionic permeants in the film with electrostatic interactions and the permeability throught the film is consequently decreased (stage 2). The electrostatic repulsion of anionic probes with the counter electrode (the cathode) in the receptor compartment may affect the decrease of permeation. When the cationic Fc^+ charges in the film are enough neutralized by anionic probes, the probe begins to overflow (stage 3). Upon reduction of the film, the charges in the film disappear and the accumulated anionic probes are released at once (stage 4). With passing time, the storage of anionic probes decreases and the permeation rate reverts to the original reduced rate (stage 5). Thus, the permeability is drastically decreased by oxidation (P_{ox2}/P_{red1} = 0.078–0.16) due to the storage of permeants in the film and is enhanced by the reduction (P_{red4}/P_{ox2} = 56–190) due to the release of the accumulated probes. The extent of the storage and release phenomena increased with increasing anionic charges in permeants (see Table III).

In the case of the permeation of cationic probes, the oxidation of the film enhances permeation or release of cationic probes compared with nonionic probes due to the electrostatic repulse with cationic Fc^+ charges in the film (stage 2). The permeability decreases gradually with time because of the decrease of the probe concentration in the film (stage 3). Upon reduction of the film, the permeability reverts to the original slow rate (stage 4). Thus, in the case of the cationic probe, the permeability enhanced relative to that of the neutral probes by oxidation due to the emphasized release by the electrostatic repulsion (P_{ox2}/P_{red1} = 10–12 in Table III).

When PMLG was cast on a Pt grid instead of PMLG–Fc(x) films and the +0.5 V potential was applied to the electrode, the permeability of the anionic NS^{2-} and cationic NA^{2+} probes slightly decreased and increased, respectively. This means that the applied potential affects partially the diffusion of ionic probes due to the ionophoresis; however, it does not play an important role for the observed storage and release phenomena of ionic probes.

Permeation and release of various anions through polypyrrole films deposited on an electrode have been reported to be changed by the positive charge formation on the film by the oxidation.[29-35] The binding and release of cationic dopamine from the polypyrrole film deposited on an electrode has been also reported to be changed by the electrochemical redox reactions.[36] These ion gate membranes of polypyrrole, however, showed slow responses, taking 5–15 min for the permeation change, and poor reproducibility because of the morphological damages of the membrane by repeated redox reactions. In contrast, our ferrocene-containing polypeptide films showed high physical stability and quick reponse for permeation, storage, and release of permeants. The micromosaic structures (fluid Fc side chain and α-helical skeleton) of polypeptide films are useful to achieve the reversible and quick responsive permeation changes.

Summary

Permeations of the water-soluble permeants through the ferrocene-containing polypeptide film could be controlled by electrochemical redox reactions of ferrocenyl side chains. The redox-sensitive permeation was explained by changes both in the hydrophilic nature of the fluid side chain region and in the content of α-helical conformations of polypeptide chains. By the introduction of long alkyl side chains with Fc groups, permeability can be controlled by both redox reactions and temperatures because of the melting of paraffin-like side-chain regions in the film. When the charged permeants were employed, the permeability could be changed complicatedly by storage and release phenomena of ionic probes in the film due to the electrostatic interaction with the cationc Fc^+ side chains. The micromosaic and heterogeneous structure (rigid helical skeleton and fluid side-chain region) of polypeptide membranes is important because vinyl polymer membranes (PFcAc) showed little permeation changes upon redox reactions on a Pt grid.

This is the first example of reversible, highly responsible permeability control of polypeptide membranes by redox reactions. We have also studied the permeability control of a redox-site-containing, multibilayer-immobilized film by electrochemical redox reactions, in which the fluidity of the lipid bilayer matrix is regulated by redox reactions

on a Pt minigrid sheet.[1,10] These electrochemically switchable films composed of lipids or polypeptides are interesting as a new type of synthetic signal-receptive membrane and as a synaptic model membrane in which a nerve impulse (electric signal) initiates the rapid release of a chemical intermediary such as acetylcholine.

Acknowledgment. This work is supported in part by Grant-in-Aid for Scientific Research form the Ministry of Education, Science and Culture.

Registry No. PFcAc, 35443-50-6; NQ_2, 97732-71-3; NS^-, 130-14-3; NS^{2-}, 1655-29-4; NS^{3-}, 5182-30-9; NA^+, 25251-63-2; NA^{2+}, 91606-37-0.

References and Notes

(1) For part 8, see: Okahata, Y.; En-na, G. *J. Chem. Soc., Perkin Trans. 2*, in press.
(2) Preliminary report: Okahata, Y.; Takenouchi, K. *J. Chem. Soc., Chem. Commun.* **1986**, 558.
(3) For a review: Okahata, Y. *Acc. Chem. Res.* **1986**, *19*, 57. *Current Topics in Polymer Science*; Ottenbrite, R. M., Utracki, L. A., Inoue, S., Eds.; Hanser: New York, 1987; Vol. 2, Chapter 6.5.
(4) Okahata, Y.; Hachiya, S.; Ariga, K.; Seki, T. *J. Am. Chem. Soc.* **1986**, *108*, 2863.
(5) Okahata, Y.; Seki, T.; Ariga, K. *J. Am. Chem. Soc.* **1988**, *110*, 2495.
(6) Okahata, Y.; Ariga, K.; Nakahara, H.; Fukuda, K. *J. Chem. Soc., Chem. Commun.* **1986**, 1069.
(7) Okahata, Y.; Ariga, K.; Shimizu, O. *Langmuir* **1986**, *2*, 538.
(8) Okahata, Y.; Taguchi, K.; Seki, T. *J. Chem. Soc., Chem. Commun.* **1985**, 1122.
(9) Okahata, Y.; Fujita, S.; Izuka, N. *Angew. Chem., Int. Ed. Engl.* **1986**, *25*, 751.
(10) Okahata, Y.; En-na, G.; Taguchi, K.; Seki, T. *J. Am. Chem. Soc.* **1985**, *107*, 5300. Okahata, Y.; En-na, G. *J. Phys. Chem.* **1988**, *92*, 4546.
(11) Okahata, Y.; Nakamura, G.; Noguchi, H. *J. Chem. Soc., Perkin Trans. 2* **1987**, 1317.
(12) Maeda, M.; Kimura, M.; Hareyama, Y.; Inoue, S. *J. Am. Chem. Soc.* **1984**, *106*, 250. Higuchi, S.; Mozawa, T.; Maeda, M.; Inoue, S. *Macromolecules* **1986**, *19*, 2263.
(13) Chung, D.; Higuchi, S.; Maeda, M.; Inoue, S. *J. Am. Chem. Soc.* **1986**, *108*, 5823.
(14) Kinoshita, T.; Yamashita, T.; Iwata, T.; Takizawa, A.; Tsujita, Y. *J. Macromol. Sci., Phys.* **1983**, *B22*, 1.
(15) Kinoshita, T.; Sato, M.; Takizawa, A.; Tsujita, Y. *J. Chem. Soc., Chem. Commun.* **1984**, 929; *Macromolecules* **1986**, *19*, 51.
(16) Takizawa, A.; Sato, M.; Kinoshita, T.; Tsujita, Y. *Chem. Lett.* **1984**, 1963.
(17) Takizawa, A.; Kinoshita, T.; Ohtani, A.; Tsujita, Y. *J. Polym. Sci., Polym. Chem. Ed.* **1986**, *24*, 665.
(18) Kinoshita, T.; Sato, M.; Takizawa, A.; Tsujita, Y. *J. Am. Chem. Soc.* **1986**, *108*, 6399.
(19) Kinoshita, T.; Iwata, T.; Takizawa, A.; Tsujita, Y. *Colloid Polym. Sci.* **1983**, *261*, 933.
(20) Okahata, Y.; Iizuka, N.; Nakamura, G.; Seki, T. *J. Chem. Soc., Perkin Trans. 2* **1985**, 1591.
(21) Lindsay, J. K.; Hauser, C. R. *J. Org. Chem.* **1957**, *22*, 355.
(22) Watanabe, J.; Ono, H.; Uematsu, I.; Abe, A. *Macromolecules* **1985**, *18*, 2141.
(23) Traverso, O.; Scandole, F. *Inorg. Chim. Acta* **1970**, *4*, 493.
(24) Sederel, W. L.; Bantjes, A.; Feijen, J. *Biopolymers* **1980**, *19*, 1603.
(25) Sandek, V.; Stokvava, S.; Schmidt, P. *Biopolymers* **1982**, *21*, 1011.
(26) Ambrose, E. J. *J. Chem. Soc.* **1950**, 3239.
(27) Watanabe, J.; Fukuda, Y.; Gehani, R.; Uematsu, I. *Macromolecules* **1984**, *17*, 1004.
(28) Watanabe, J.; Ono, H. *Macromolecules* **1986**, *19*, 1079.
(29) Burgmayer, P.; Murray, R. W. *J. Am. Chem. Soc.* **1982**, *104*, 6139.
(30) Burgmayer, P.; Murray, R. W. *J. Phys. Chem.* **1984**, *88*, 2515.
(31) Shinohara, H.; Aizawa, M.; Shirakawa, H. *J. Chem. Soc., Chem. Commun.* **1986**, 87; *Chem. Lett.* **1985**, 179.
(32) Aizawa, M.; Watanabe, S.; Shinohara, H.; Shirakawa, H. *J. Chem. Soc., Chem. Commun.* **1985**, 264.
(33) Shimizu, T.; Ohtani, A.; Iyoda, T.; Honda, K. *J. Chem. Soc., Chem. Commun.* **1986**, 1415.
(34) Iyoda, T.; Ohtani, A.; Shimizu, T. *Chem. Lett.* **1986**, 687.
(35) Zinger, B.; Miller, L. L. *J. Am. Chem. Soc.* **1984**, 106, 6861.
(36) Miller, L. L.; Zhou, Q. X. *Macromolecules* **1987**, *20*, 1594.

Excimer Kinetics in Copolymers Containing Isolated Pairs of Chromophores

David A. Holden,* Ali Safarzadeh-Amiri, Charles P. Sloan, and Paul Martin

Guelph–Waterloo Centre for Graduate Work in Chemistry, Department of Chemistry, University of Waterloo, Waterloo, Ontario, Canada N2L 3G1. *Received February 2, 1988; Revised Manuscript Received April 29, 1988*

ABSTRACT: Side-chain cyclization in polymers was studied by observing the kinetics of excimer formation and decay in copolymers containing approximately 1% of bis[ω-(1-naphthyl)alkyl] esters of fumaric or itaconic acids. In the fumarate copolymer series the relative intensity of excimer fluorescence decreased with increasing number of CH_2 groups between the naphthalene chromophore and the ester linkage. Only 20–40% of starting conformations cyclized to give excimer during the singlet lifetime, with a rate constant of 5×10^7 to 5×10^8 s^{-1}, depending on solvent and temperature. The remainder decayed with the same lifetime as a monomeric model compound. In the itaconate ester copolymers the fraction of cyclizing monomer species was considerably smaller, but the rate of cyclization was comparable to that observed for the fumarate copolymers. Studies on a variety of bichromophoric model compounds showed that the geometry at the central C–C bond has a pronounced effect on the fraction of chromophore pairs capable of reaching the excimer configuration.

Introduction

The reaction between groups attached to a polymer chain is an important class of physical phenomenon, with relevance to chain branching, ring formation, and intramolecular catalysis.[1,2] Photophysical studies on model polymers can provide fundamental information on such intrachain reactions, provided the model system is carefully designed. An example is the use of excimer and exciplex formation by Winnik and co-workers to study the rates of end-to-end chain cyclization in polymers.[3] In order to create a well-defined model system the University of Toronto group had to achieve quantitative labeling of both ends of monodisperse polymers with chromophoric groups.

A related problem which has received little attention in the literature is the process of side-chain cyclization,[4] illustrated in Figure 1. We define side-chain cyclization

0024-9297/89/2222-0315$01.50/0